Article

Discovery Medicine 2025; 37(199): 1479–1492
https://doi.org/10.24976/Discov.Med.202537199.129

Piezo1 Activates the PI3K/Akt Pathway to Stimulate Osteogenic Differentiation of Bone Marrow Mesenchymal Stem Cells and Speed Up Fracture Healing

Shengkai Mu[1], Xuanlu Qi[2], Haixia Hong[3], Honglai Tian[3,*]

[1]Department of Orthopedics, Hospital of Traditional Chinese Medicine Liaocheng City, 252000 Liaocheng, Shandong, China
[2]Department of Orthopedics, Hospital of Traditional Chinese Medicine Heze City, 274000 Heze, Shandong, China
[3]Department of Orthopedics, Affiliated Hospital of Shandong University of Traditional Chinese Medicine, 250014 Jinan, Shandong, China
*Correspondence: tianhlai@163.com (Honglai Tian)
Published: 20 August 2025

Background: Bone healing is a complex biological process influenced by various cellular and molecular factors. Piezo-type mechanosensitive ion channel component 1 (Piezo1) is closely associated with function of bone cells. This study aims to investigate the effects of Piezo1 on bone healing, specifically examining its ability to enhance the growth and osteogenic differentiation of bone marrow-derived mesenchymal stem cells (BM-MSCs), as well as assessing its effect on the Phosphoinositide 3-kinase/Protein kinase B (PI3K/AKT) signaling pathway.

Methods: This study utilized a rat fracture model to evaluate the effects of rat Piezo1 recombinant proteins on bone healing. Micro-computed tomography (Micro-CT) scans were performed during weeks 6 and 8 after fracture to assess the formation of callus during the healing process, including trabecular thickness (Tb.Th), trabecular number (Tb.N), and bone mineral density (BMD). The serum levels of alkaline phosphatase (ALP) and transforming growth factor beta 1 (TGF-β1) were evaluated using an enzyme-linked immunosorbent assay. Histological evaluation included hematoxylin–eosin staining to examine tissue composition and quantitative analysis of bone morphogenetic protein (BMP)-2 expression through immunohistochemistry. Furthermore, BM-MSCs were treated with different doses of Piezo1, and cell viability was assessed using the Cell Counting Kit-8 (CCK-8) assay. ALP staining and alizarin red staining were conducted to evaluate osteogenic differentiation. Additionally, the expression levels of osteogenic markers and the activation of the PI3K/AKT signaling pathway were examined using Western blot analysis.

Results: Piezo1 significantly enhanced trabecular bone formation in a rat fracture model, with micro-CT analysis showing amplified callus formation and improved Tb.Th, Tb.N, and BMD at weeks 6 and 8 ($p < 0.05$). The serum levels of ALP and TGF-β1 were elevated in the Piezo1 group ($p < 0.05$). Histological evaluation revealed more mature bone in the Piezo1 group than in the fracture group, especially by week 8, along with increased BMP-2 expression ($p < 0.05$). *In vitro*, CCK-8 assays indicated that Piezo1 promoted BM-MSC growth in a dose- and exposure duration-dependent manner ($p < 0.05$). After 7 days of osteogenic differentiation, ALP and alizarin red staining showed enhanced osteogenic activity and calcium deposition in Piezo1-treated cells ($p < 0.05$). Western blot analysis confirmed increased expression of osteogenic markers in treated BM-MSCs, and Piezo1 activated the PI3K/AKT signaling pathway by increasing the phosphorylation levels of PI3K and AKT ($p < 0.05$).

Conclusions: Piezo1 significantly enhances the growth and osteogenic differentiation of BM-MSCs, accelerating bone healing by activating the PI3K/AKT signaling pathway and increasing osteogenic marker expression. These findings support the potential use of Piezo1 as a bone healing enhancer.

Keywords: Piezo1; fracture healing; BM-MSCs; osteoblast differentiation

Introduction

Fractures are common clinical injuries, with a complex healing process which is influenced by various factors [1–3]. Bone healing progresses through four stages: inflammation, cartilaginous callus formation, ossification, and remodeling [4,5]. Delays in these stages can lead to poor healing or complications [6]. In recent years, there has been substantial focus in orthopedic research on identifying effective bone healing promoters.

Piezo-type mechanosensitive ion channel component 1 (Piezo1), a mechanically sensitive ion channel, responds to external mechanical stimuli, such as stretch and compression, by modulating intracellular calcium ion concentrations through changes in cell membrane permeability [7,8]. This process is crucial for cell signaling, gene expression, and cell fate determination [9]. Piezo1 activation is closely related to the bone cell function, including key processes such as bone formation, bone resorption, and osteoblast differentiation (the process by which mesenchymal

stem cells develop into osteoblasts, the bone-forming cells) [10]. During fracture healing, the mechanical sensing and response of cells are essential for promoting the proliferation, migration, and differentiation of bone cells, processes that may be modulated by the Piezo1 channel [11]. Previous studies have revealed that Piezo1 stimulates osteoblast growth and differentiation, thereby supporting bone formation by modulating the expression of factors involved in bone metabolism [12,13]. In bone biology, Piezo1 plays a vital role in promoting osteoblast proliferation, differentiation, and migration, thereby contributing significantly to bone formation, resorption, and fracture repair. It serves as a crucial mediator linking mechanical signals to the regulation of bone metabolism.

Various extracellular signals, including growth factors, cytokines, and mechanical stimuli activate the Phosphoinositide 3-kinase/Protein kinase B (PI3K/AKT) axis. Once activated, this pathway mediates several cellular functions, such as survival, proliferation, migration, and differentiation [14,15]. PI3K/AKT signaling has been reported to promote osteoblast proliferation, enhance the osteogenic differentiation of mesenchymal stem cells (MSCs), and accelerate matrix mineralization [16]. Furthermore, this pathway plays an essential role in angiogenesis, which is crucial for effective fracture healing.

Additionally, other biological molecules, such as transforming growth factor beta (TGF-β) and bone morphogenetic proteins (BMPs), also play crucial roles in bone healing [17,18]. TGF-β is vital for osteoblast differentiation, while BMPs are key factors that promote osteogenic differentiation [19,20]. Therefore, the effects of Piezo1 on these factors may represent one of the underlying mechanisms by which it promotes bone healing.

This study aims to investigate the impact of Piezo1 on bone fracture healing, particularly examining its role in trabecular formation, mineralization, and the associated biochemical markers. Using a rat fracture model, this study assesses the effectiveness of Piezo1 in promoting bone healing and elucidates its underlying mechanisms. The findings of this are anticipated to form the basis for translating Piezo1 research into clinical practice as an adjuvant for bone healing, potentially resulting in the development of novel enhancers for bone repair.

Materials and Methods

Establishment of Fracture Model

Wistar rats (n = 12), aged 12 weeks old and weighing 400–420 g, were obtained from Charles River (Beijing, China). They were housed under controlled conditions with a temperature ranging from 20 °C to 24 °C, relative humidity of 50%–60%, and a 12 h light–dark cycle. To induce general anesthesia, a 3% sodium pentobarbital (40 mg/kg) was administered via intraperitoneal injection, ensuring that the rats were in a completely pain-free state. The rats were then positioned supine on the surgical table. A 2–3 cm incision was made lengthwise on the upper thigh, and subcutaneous tissue was separated to expose the femur. A transverse fracture was then created at the proximal femur using a specialized fracture clamp. The fracture ends were aligned and fixed using a steel pin. The subcutaneous tissue and skin were sutured in layers to minimize the risk of infection. Postoperative wound healing was regularly monitored. This protocol involving animal experiments was approved by the Institutional Animal Care and Use Committee of Shandong Academy of Pharmaceutical Sciences (IACUC-care-2024024) and was conducted following the Guide for the Care and Use of Laboratory Animals, 8th edition (National Research Council (NRC), 2010).

Before all surgical procedures, rats were anesthetized with an intraperitoneal injection of 3% pentobarbital sodium (40 mg/kg). Postoperative analgesia was provided with meloxicam (1–2 mg/kg/day) for 3 consecutive days to alleviate postoperative pain. The fracture model was successfully established in all rats. After surgery, the rats were monitored daily for signs of pain, infection, or abnormal behavior, and appropriate interventions were taken as needed. Surgical wounds were kept clean and disinfected to reduce the risk of infection. Rats experiencing severe stress responses or complications during the experiment were humanely euthanized according to predetermined humane endpoints. At scheduled time points, euthanasia was performed using CO_2 inhalation followed by cervical dislocation to ensure a painless death.

Drug Treatment

The rats were randomly assigned to two groups: a fracture group (n = 6) and a rat Piezo1 treatment group (n = 6). Each group was administered saline (equal volume) and Piezo1 recombinant proteins (100 mg/kg) (Purity >90%, R3227m, EIAab, Wuhan, China) via gavage once daily for 8 weeks. The dosage of Piezo1 recombinant protein was determined based on the results from dose-ranging screening in our preliminary experiments. Drug administration was initiated on the second day after successful model establishment. At scheduled time points, euthanasia was performed using CO_2 inhalation followed by cervical dislocation to ensure a painless death. The fracture healing sites were then collected for subsequent experiments.

Micro-CT Analysis

At 6 and 8 weeks, micro-computed tomography (micro-CT) scanning (SkyScan 1176, Bruker, Billerica, MA, USA) was performed to analyze the proximal femoral fracture ends in each rat group. Following the scan, software was used to reconstruct three-dimensional images of the fracture sites and analyze the bone structure.

Hematoxylin-Eosin (HE) Staining

The rat fracture tissue was collected and fixed in 10% neutral buffered formalin for 24 hours. Tissue was then decalcified in 10% EDTA solution for 2 weeks, with regular monitoring of the decalcification process. After decalcification, the tissue underwent dehydration using a graded ethanol series, with each step lasting 1 hour, followed by clearing in xylene twice for 30 minutes each. The tissue was embedded in paraffin and sectioned into 5 µm-thick slices, which were mounted onto glass slides and heat-fixed. The sections were deparaffinized with xylene and rehydrated through a graded ethanol series to distilled water. Hematoxylin staining (C0105S, Beyotime, Shanghai, China) was applied for 5 minutes, followed by a water rinse, differentiation in 1% hydrochloric acid ethanol, and bluing. Then the sections were stained with 1% eosin (C0105S, Beyotime, Shanghai, China) for 5 minutes, rinsed with water, dehydrated through a graded ethanol series, cleared in xylene, and mounted with neutral resin. Once dried, the slides were processed for histopathological analysis using a BX53 microscope (Olympus, Tokyo, Japan).

The scoring criteria were as follows: a score of 0 indicated only fibrous tissue with no bone formation; 1 indicated predominantly fibrous tissue with a small amount of cartilage; 2 indicated mainly cartilaginous tissue with initial signs of bone formation; 3 indicated evident ossification with a predominance of immature (woven) bone; and 4 indicated mature bone tissue, with minimal or no fibrous or cartilaginous tissue, reflecting good fracture healing.

The scoring was performed independently in a blinded manner by two experienced pathologists. For each section, 3–5 fields of view were randomly selected, and the average score was calculated. Higher scores reflected a better degree of fracture healing.

Immunohistochemistry (IHC)

Tissue samples from the fracture healing site were extracted and fixed in 4% paraformaldehyde for 24-hour. Then, the samples were dehydrated through a series of ethanol concentrations, cleared, and embedded in paraffin. Once the paraffin solidified, tissues were sectioned into 5 µm-thick slices. The sections were mounted flat on glass slides and baked in an oven at 60 °C for 1 hour to fix them. Subsequently, the slides were placed in xylene to remove the paraffin, followed by hydration through a graded ethanol concentration (100%, 95%, 80%, and 70%). After that, the tissue sections were blocked with 5% BSA and incubated overnight at 4 °C with a specific primary antibody targeting BMP-2 (1:1000, bs-1012R, Funakoshi, Tokyo, Japan), followed by three PBS washes. The following day, the sections were incubated for 1 hour with the appropriate secondary antibody (1:1000, ab6728, Abcam, Cambridge, UK) and washed with PBS. The sections were then stained using DAB chromogen, dehydrated through 70%, 80%, 95%, and 100% ethanol, cleared with xylene, and mounted with neutral gum. The stained sections were examined under a light microscope (BX53, Olympus, Tokyo, Japan) to evaluate BMP-2 expression in the fracture healing tissue. The IHC images were quantitatively analyzed using ImageJ software (version 1.5f, National Institutes of Health, Bethesda, MD, USA).

Determination of Alkaline Phosphatase (ALP) and TGF-β1 Concentrations

Blood samples were collected from rats via tail vein puncture during weeks 6 and 8 post-fracture. The blood was then centrifuged, and the resultant serum sample was stored at –80 °C. Meanwhile, ALP (YS03147B) and TGF-β1 (YS05620B) assay kits were purchased from YaJi Biological (Shanghai, China).

ALP assay reagents were prepared following the manufacturer's instructions, and serum samples were appropriately diluted. The substrate and buffer were mixed and incubated at 37 °C for a specified duration. After the reaction was terminated, the absorbance was determined using a microplate reader (EnVision, PerkinElmer, Waltham, MA, USA) at 405 nm, and ALP activity (U/L) was calculated.

For the TGF-β1 assay, the capture antibody was coated onto the plate, followed by the addition of diluted serum samples and detection antibodies. After washing the plate, the substrate was added, and the reaction was terminated. Finally, the absorbance was determined at 450 nm to calculate the TGF-β1 concentration (pg/mL).

Cultivation of Rat Bone Marrow-derived Mesenchymal Stem Cells (BM-MSCs) and Induction of Osteogenic Differentiation

Rat BM-MSCs (RAT-iCell-s018) were purchased from Cellverse Co., Ltd. (Shanghai, China). The cells were centrifuged, resuspended in a culture medium containing FBS and penicillin-streptomycin, and then seeded into culture flasks. The cells were incubated at 37 °C with 5% CO_2 and the medium was replaced regularly. The induction medium was prepared containing 10% FBS, 1% penicillin–streptomycin, 10 mM β-glycerophosphate, 100 nM dexamethasone, and 50 µg/mL of vitamin C. Mesenchymal stem cells (2×10^5 cells/well) were seeded in the induction medium and cultured at 37 °C with 5% CO_2. The medium was changed every 2 days to maintain cell growth and differentiation, and the induction process lasted for 7 days.

Piezo1 was dissolved in DMSO to prepare a high-concentration stock solution of 10 mM. The stock solution was diluted with a serum-free or low-serum medium to achieve the desired working concentration. Prior to the formal experiments, preliminary studies were conducted to determine the optimal Piezo1 concentration (0.1–10 µM) for *in vitro* use. The concentration of Wortmannin (0.1 µM) was determined based on preliminary experiments conducted in our laboratory, which aimed to identify the optimal dose that effectively inhibits PI3K activity with-

out significant cytotoxicity. During the cultivation of BM-MSCs and the induction of osteogenic differentiation, different concentrations of Piezo1 (0, 0.1, 1, 5, and 10 μM) or Piezo1 (5 μM) + Wortmannin (0.1 μM) (HY-10197, MedChemExpress, Monmouth Junction, NJ, USA) were applied for treatment. The density of cells during induction, differentiation, and expansion was 15,000 cells/cm^2. Before using this study, the cells underwent species identification and the mycoplasma testing.

Cell Counting Kit-8 (CCK-8) Assay

Cultured BM-MSCs were passaged into culture flasks and incubated until they achieved approximately 80% confluence. The cells were then digested with trypsin, counted, and the cell concentration was adjusted to an appropriate seeding density (1×10^4 cells/mL). Different concentrations of Piezo1 (0, 0.1, 1, 5, and 10 μM) or other reagents were added to their respective groups of cells, and the cells were cultured for an additional 24 hours. After that, 10 μL of CCK-8 reagent (C0038, Beyotime, Shanghai, China) was added to each well, mixed gently, and incubated at 37 °C for 1 hour. The absorbance of each well was determined at 450 nm using a microplate reader (Multiskan Sky, Thermo Fisher Scientific, Waltham, MA, USA). The effects of different treatment conditions on BM-MSC activity were analyzed. Cell viability was computed using the following formula: Cell viability (%) = (OD experiment – OD blank)/(OD control – OD blank) × 100%.

5-ethynyl-2′-deoxyuridine (EdU) Staining

EdU Cell Proliferation Detection Kit (C0071S, Beyotime, Shanghai, China) was used for staining. During the experiment, EdU working solution was first added to the cell culture medium and incubated for 2 hours, allowing EdU to incorporate into the newly synthesized DNA of proliferating cells. Subsequently, the cells were washed with PBS and fixed with 4% paraformaldehyde for 15 minutes, followed by a 20-minute treatment with 0.5% Triton X-100 to increase cell permeability. The Click reaction mixture was prepared following the kit instructions and added to the cells for a 30-minute incubation in the dark, enabling a specific chemical reaction between EdU and the fluorescent azide dye. After the reaction, the cell nuclei were optionally counterstained with DAPI (C0065, Solarbio, Beijing, China). Finally, the proportion of EdU-positive cells was observed and analyzed under a fluorescence microscope (BX53, Olympus, Tokyo, Japan) to evaluate cell proliferation, and fluorescence-stained images were quantitatively analyzed using ImageJ software (version 1.5f, National Institutes of Health, Bethesda, MD, USA).

ALP Staining

After 7 days of osteogenic differentiation induction of BM-MSCs, the cells were fixed with 4% paraformaldehyde for 10 minutes and washed 3 times with PBS to remove the fixative. The ALP staining working solution (C3206, Beyotime, Shanghai, China) was prepared following the kit instructions and handled under light-protected conditions. The staining solution was added to the cells and incubated in the dark for 30 minutes, with the staining effect being observed periodically. After that, the cells were washed 3 times with PBS or distilled water to terminate the reaction. The staining results were observed under a microscope (BX53, Olympus, Tokyo, Japan), with ALP-positive cells exhibiting a purple-blue precipitate. The staining images were quantitatively analyzed using ImageJ software (version 1.5f, National Institutes of Health, Bethesda, MD, USA).

Alizarin Red Staining

An alizarin red staining solution was prepared, typically using a 0.1% alizarin red solution (pH 4.2). The staining solution (C0138, Beyotime, Shanghai, China) was added to the fixed cells and incubated at room temperature for 5 minutes. The cells were gently washed with distilled water to remove any unbound dye. The orange mineralized nodules were observed using an inverted microscope (BX53, Olympus, Tokyo, Japan), and images were recorded. Finally, the staining images were quantitatively analyzed using ImageJ software (version 1.5f, National Institutes of Health, Bethesda, MD, USA).

Western Blot Analysis

Total protein was extracted from the cells using the RIPA lysis buffer. The mixture was centrifuged to remove cell debris, and protein was quantified. The extracted protein was mixed with the loading buffer, boiled to denature the protein, and resolved using SDS-PAGE. After separation, the proteins were transferred onto a PVDF membrane, which was blocked with 5% BSA to minimize nonspecific binding. The membrane was then incubated overnight at 4 °C with the following specific primary antibodies: BMP-2 (1:1000, ab284387, Abcam, Cambridge, UK), ALP (1:1000, ab307726, Abcam, Cambridge, UK), Collagen Type I (COL-1) (1:1000, ab270993, Abcam, Cambridge, UK), Osteocalcin (OCN) (1:1000, ab309521, Abcam, Cambridge, UK), Osteopontin (OPN) (1:1000, ab214050, Abcam, Cambridge, UK), Runx2 (1:1000, ab192256, Abcam, Cambridge, UK), Phosphorylated AKT (p-AKT) (1:1000, AA329, Beyotime, Shanghai, China), AKT (1:1000, AA326, Beyotime, Shanghai, China), Phosphorylated Phosphoinositide 3-Kinase (p-PI3K) (1:1000, PA5-17387, Thermo Fisher Scientific, Waltham, MA, USA), PI3K (1:1000, MA5-14870, Thermo Fisher Scientific, Waltham, MA, USA), and Glyceraldehyde-3-Phosphate Dehydrogenase (GAPDH) (1:1000, MA5-15738, Thermo Fisher Scientific, Waltham, MA, USA), typically. The next day, the membrane was washed with PBS and incubated with HRP-conjugated secondary antibodies (1:1000, A0208, Beyotime, Shanghai, China) or (1:1000, ab205719,

Abcam, Cambridge, UK) at 25 °C for 1 hour, and then washed again. A gel imaging system (ChemiDoc MP, Bio-Rad, Hercules, CA, USA) was used to capture the signals on the membrane, and the band intensity was analyzed using Image J software (version 1.5f, National Institutes of Health, Bethesda, MD, USA) to determine the expression level of the target protein.

Statistical Analysis

Data were analyzed using GraphPad Prism software (version 9.0, GraphPad Software Inc., San Diego, CA, USA). Student's *t*-test was applied for comparisons between two groups, while one-way ANOVA, followed by post hoc tests, was used for comparisons among multiple groups. The Shapiro-Wilk test was applied to assess data normality before performing parametric analyses. The data were expressed as mean ± standard deviation, with a *p*-value of <0.05 considered statistically significant.

Results

Piezo1 Promotes Trabecular Bone Formation

We evaluated the callus tissue of the rats through micro-CT scans. Compared to the fracture group, the Piezo1 group showed significantly more callus tissue in weeks 6 and 8, with a greater number of denser trabeculae and increased mineralization (Fig. 1a). The Piezo1 group demonstrated increased trabecular thickness (Tb.Th), trabecular number (Tb.N), and bone mineral density (BMD) at both weeks 6 and 8 compared with the fracture group (Fig. 1b–d). In contrast, trabecular separation (Tb.Sp) in the Piezo1 group was substantially lower than in the fracture group (Fig. 1e).

Piezo1 Improves the Histological Scores of Fracture Healing in Rats

Furthermore, we assessed serum ALP and TGF-β1 levels in rats. As shown in Fig. 2a–d, the Piezo1 group had significantly elevated ALP and TGF-β1 levels at weeks 6 and 8 compared to the fracture group ($p < 0.05$). HE staining revealed that the fracture group exhibited more fibrous and cartilaginous tissue at week 6, with no immature bone tissue present (Fig. 2e). By week 8, the fibrous tissue in the fracture group had been gradually replaced with bone tissue, with some mature bone observed. In contrast, the Piezo1 group showed a more mature bone tissue by week 8.

Additionally, we also assessed BMP-2 expression in the callus tissue through IHC (Fig. 2f). In the fracture group, BMP-2 levels were lowest in week 6 but increased by week 8. The Piezo1 group exhibited significantly higher BMP-2 staining at weeks 6 and 8, with the highest level of BMP-2 staining observed at week 8. Fig. 2g,h presents the histopathological scores, where the Piezo1 group had substantially higher scores than the fracture group at both weeks 6 and 8 ($p < 0.05$). The quantitative analysis of BMP-2 expression (Fig. 2i,j) revealed that BMP-2 levels in the Piezo1 group were notably higher than in the fracture group at both weeks 6 and 8 ($p < 0.05$).

Piezo1 Promotes the Growth and Osteogenic Differentiation of BM-MSCs

The activity of BM-MSCs treated with different concentrations of Piezo1 was evaluated using the CCK-8 assay. We observed that compared to the 0 µm group, the activity of BM-MSCs in the Piezo1-treated groups (0.1, 1, and 5 µm) increased over time and concentration, demonstrating a clear dose- and time-dependent effect (Fig. 3a). However, the activity of BM-MSCs treated with a higher concentration (10 µm) of Piezo1 significantly decreased compared to the 5 µm group, indicating that high doses of Piezo1 exerted cytotoxicity on BM-MSCs ($p < 0.05$). On day 7 of BM-MSC growth, the cell activity in the Piezo1-treated groups (0.1, 1, 5, and 10 µm) was significantly higher than of the 0 µm group ($p < 0.05$) (Fig. 3a). Therefore, 5 µm Piezo1 was selected for further experiments. After 7 days of osteogenic induction of BM-MSCs, ALP and alizarin red staining were performed. As illustrated in Fig. 3b–e, the levels of ALP and alizarin red staining in the Piezo1 group were notably higher than those in the control group ($p < 0.05$).

We also evaluated the effect of Piezo1 on the expression of osteogenic markers in BM-MSCs using Western blot analysis. The Piezo1 treatment significantly increased the protein expression levels of ALP, COL-1, OCN, OPN, and Runx2 in BM-MSCs (Fig. 4a–f; $p < 0.05$).

Piezo1 Activates the PI3K/AKT Signaling Pathway in BM-MSCs

As shown in Fig. 5a–c, the phosphorylation levels of PI3K and AKT were significantly higher in Piezo1-treated BM-MSCs than in the control group ($p < 0.05$). To further investigate whether Piezo1 regulates osteogenic differentiation of BM-MSCs via the PI3K/AKT signaling pathway, cells were treated with the PI3K/AKT signaling pathway inhibitor Wortmannin. As illustrated in Fig. 5d–f, Wortmannin treatment significantly suppressed the protein expression levels of p-PI3K/PI3K, p-AKT/AKT ($p < 0.05$).

Piezo1 Promotes the Proliferation and Osteogenic Differentiation of BM-MSCs by Activating the PI3K/AKT Signaling Pathway

As shown in Fig. 6a,b, the number of EdU-positive BM-MSCs was significantly reduced in the Piezo1 + Wortmannin group compared to the Piezo1 group. Furthermore, ALP staining and Alizarin Red staining revealed that both ALP activity and mineralized nodule formation were substantially decreased in the Piezo1 + Wortmannin group compared to the Piezo1-treated group (Fig. 6c–f; $p < 0.05$).

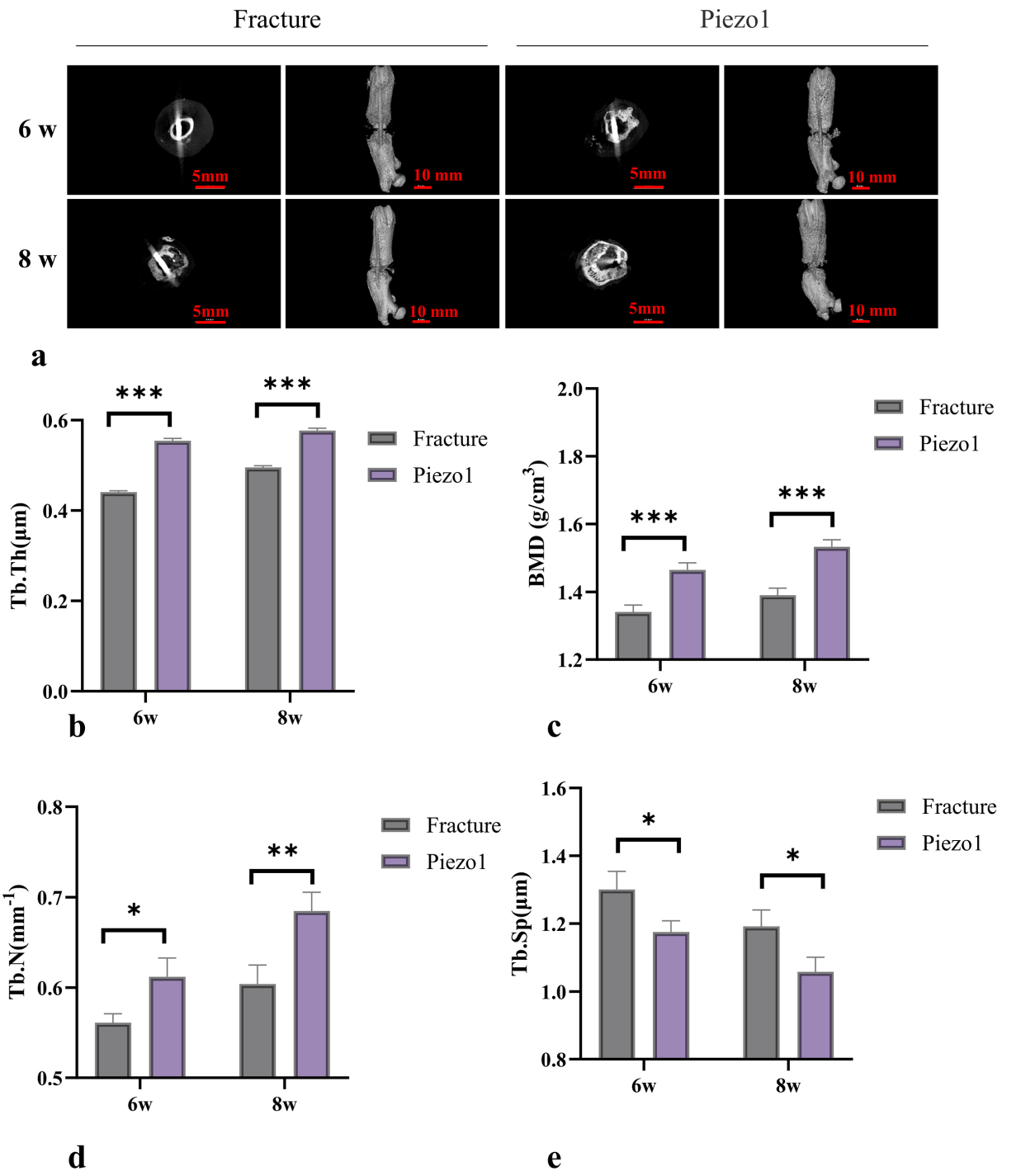

Fig. 1. Piezo-type mechanosensitive ion channel component 1 (Piezo1) promotes trabecular bone formation. (a) Micro-computed tomography (micro-CT) images of trabecular bone in the proximal femur fracture region of rats. (b) Micro-CT analysis measuring trabecular thickness (Tb.Th). (c) Bone mineral density (BMD). (d) Trabecular number (Tb.N). (e) Trabecular separation (Tb.Sp). n = 3. *$p < 0.05$, **$p < 0.01$, ***$p < 0.001$.

Piezo1 Enhances the Expression of Osteogenic Genes in BM-MSCs by Activating the PI3K/AKT Signaling Pathway

Fig. 7a–f demonstrates that treatment with Wortmannin substantially suppressed the protein levels of ALP, COL-1, OCN, OPN, and Runx2 compared to the Piezo1 group ($p < 0.05$), indicating that inhibition of the PI3K/AKT pathway attenuates Piezo1-induced osteogenic differentiation.

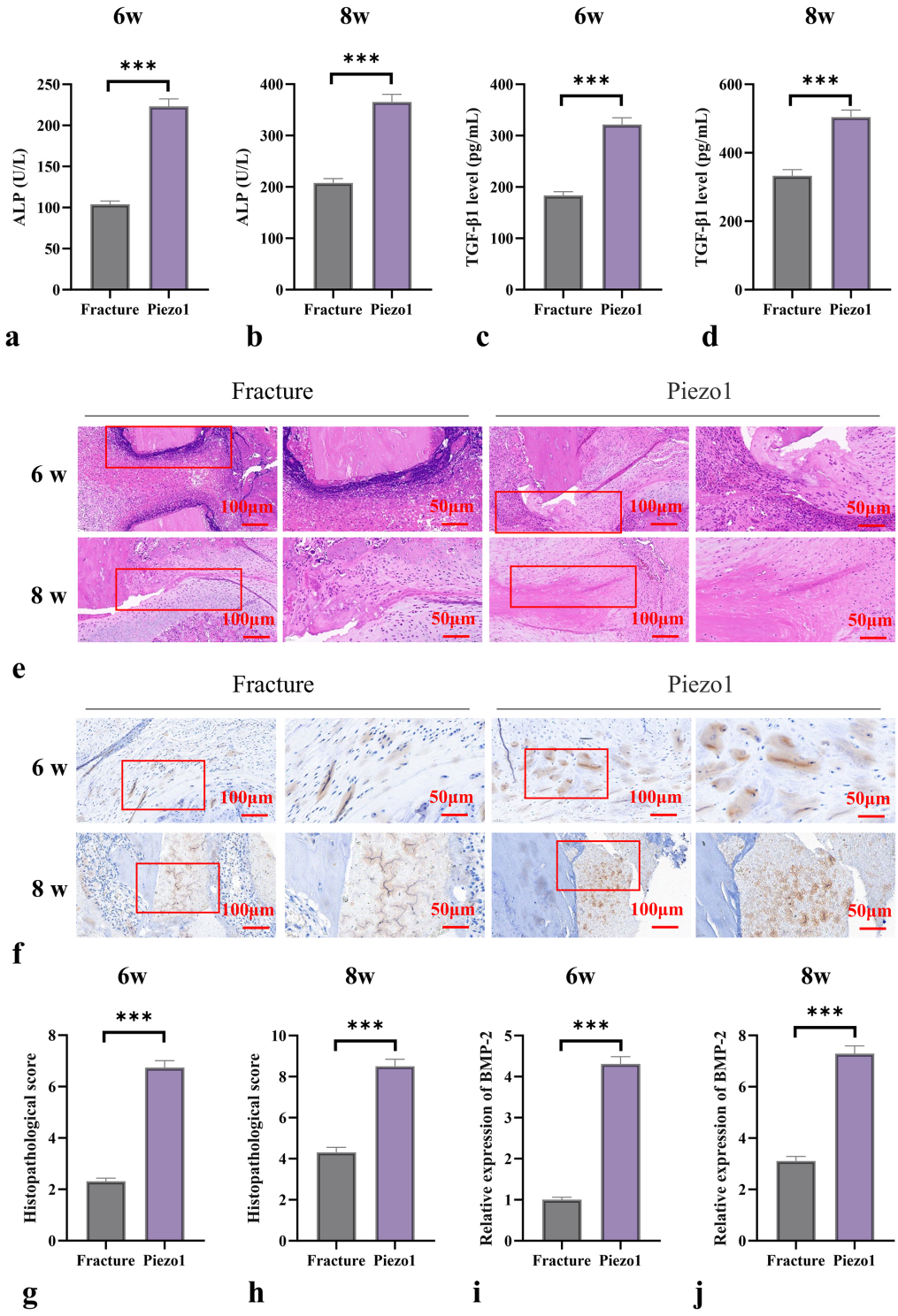

Fig. 2. Piezo1 improves the histological scores of fracture healing in rats. (a) Effect of Piezo1 on alkaline phosphatase (ALP) levels in rats at week 6 of fracture healing. (b) Effect of Piezo1 on ALP levels in rats at week 8 of fracture healing. (c) Effect of Piezo1 on transforming growth factor beta 1 (TGF-β1) levels in rats at week 6 of fracture healing. (d) Effect of Piezo1 on TGF-β1 levels in rats at week 8 of fracture healing. The red framework indicates the magnified area. (e) Hematoxylin-eosin (HE) staining of fracture healing tissue in rats at weeks 6 and 8 after Piezo1 treatment. The red framework indicates the magnified area. (f) Immunohistochemistry (IHC) of bone morphogenetic protein (BMP)-2 in the healing tissue of rats at weeks 6 and 8 after Piezo1 treatment. (g) Histopathological score of fracture healing tissue at week 6 in rats. (h) Histopathological score of fracture healing tissue at week 8 in rats. (i) Quantitative analysis of BMP-2 expression in callus tissue at week 6 using IHC after Piezo1 treatment. (j) Quantitative analysis of BMP-2 expression in callus tissue at week 8 using IHC after Piezo1 treatment. n = 3. ***$p < 0.001$.

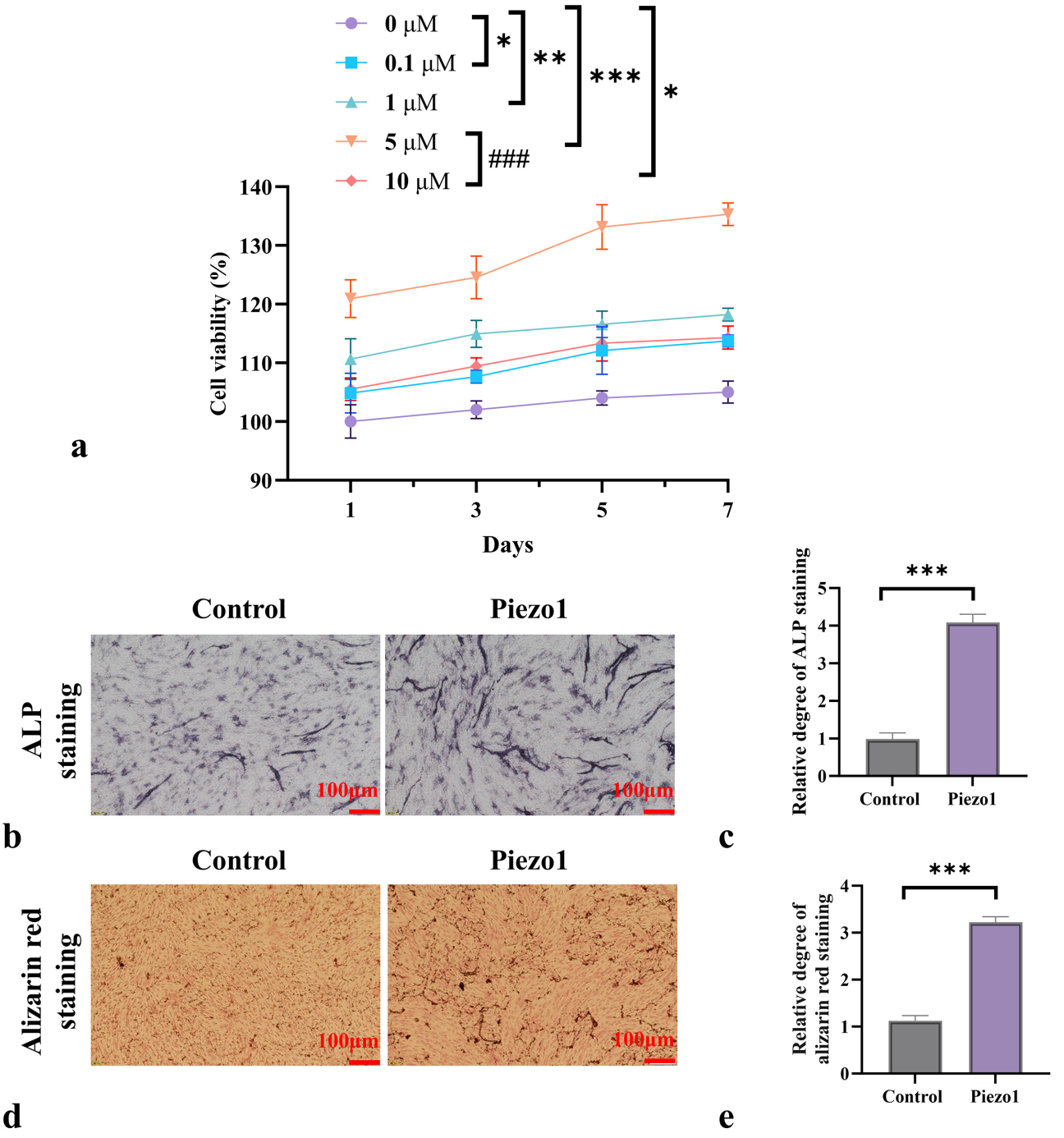

Fig. 3. Piezo1 promotes the growth and osteogenic differentiation of bone marrow-derived mesenchymal stem cells (BM-MSCs). (a) Effect of different concentrations of Piezo1 on BM-MSCs activity. (b,c) ALP staining to assess the effect of Piezo1 on the osteogenic capability of BM-MSCs after 7 days of osteogenic induction. (d,e) Alizarin red staining to assess the effect of Piezo1 on calcium deposition levels in BM-MSCs after 7 days of osteogenic induction. n = 3. $^{*}p < 0.05$, $^{**}p < 0.01$, $^{***}p < 0.001$, $^{\#\#\#}p < 0.001$.

Discussion

Previous studies have shown that Piezo1 stimulates osteoblast growth and differentiation, supporting bone formation by modulating the expression of factors involved in bone metabolism [12,13]. Contrary to these studies [12,13], which primarily focused on Piezo1 activation through mechanical stimulation, our study is the first, to our knowledge, to demonstrate that exogenous delivery of recombinant Piezo1 protein directly enhances osteogenic differentiation of BM-MSCs by activating the PI3K/AKT signaling pathway, independent of mechanical stimuli.

This study provides a comprehensive investigation of the role of Piezo1 in promoting bone fracture healing, of-

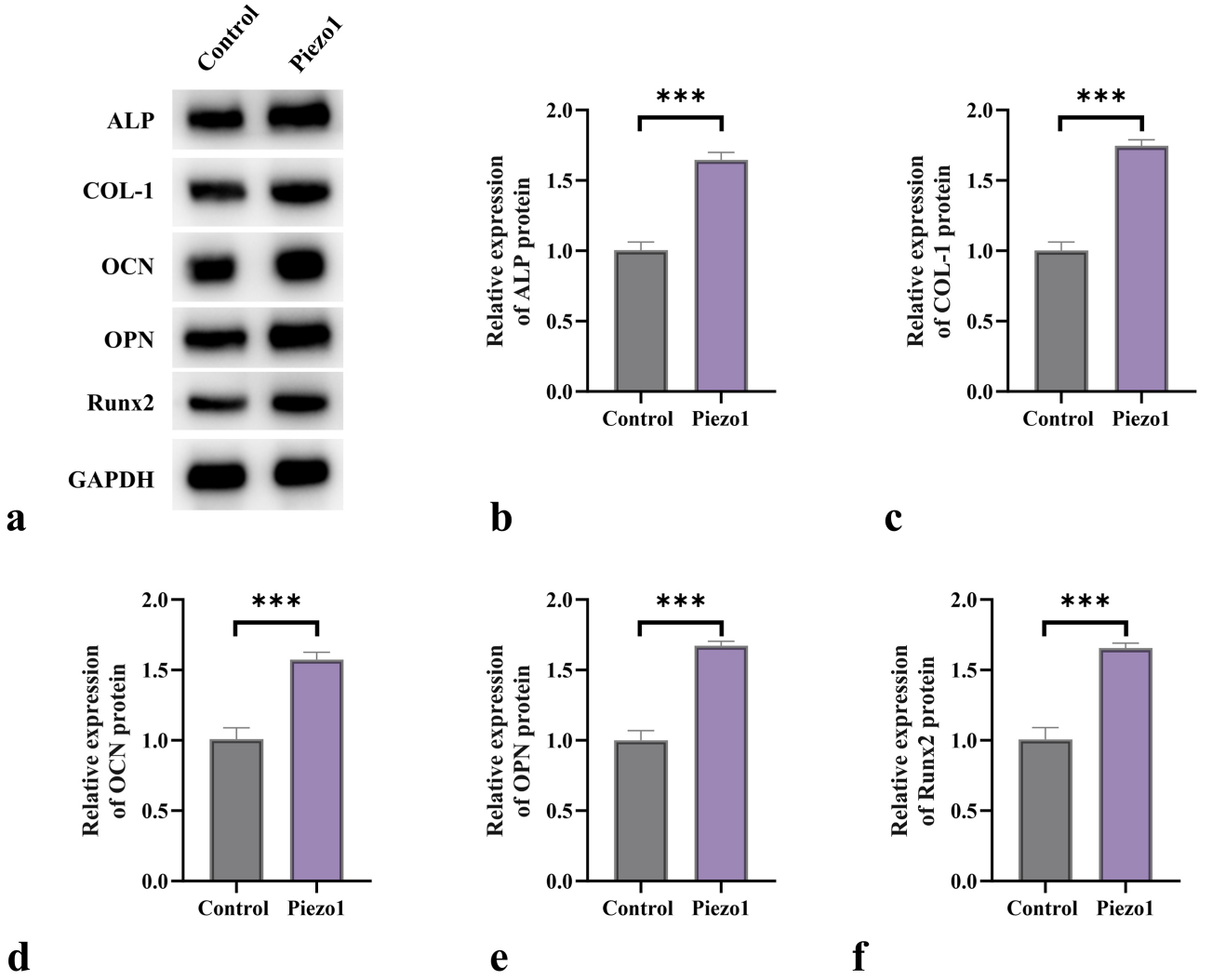

Fig. 4. Piezo1 increases the expression of osteogenic factors in BM-MSCs. (a–f) Effect of Piezo1 on the protein expression levels of alkaline phosphatase (ALP), Collagen Type I (COL-1), Osteocalcin (OCN), Osteopontin (OPN), and Runx2 in BM-MSCs. n = 3. ***$p < 0.001$.

fering significant experimental data to support its potential as an adjuvant for bone healing. Through micro-CT scanning, we found that the Piezo1 group exhibited a substantially greater amount of callus tissue in weeks 6 and 8, with increased values for Tb.Th, Tb.N, and BMD than in the fracture group. These findings are consistent with those of Kang *et al*. [21], which indicated that Piezo1 promotes the proliferation and differentiation of osteoblasts, underscoring its significance in regulating bone metabolism. During fracture healing, BMD and trabecular thickness (Tb.Th) are important indicators for evaluating the quality and mechanical stability of newly formed bone. BMD reflects the mineral deposition per unit volume and is directly correlated with the strength and fracture resistance of bone tissue. Tb.Th indicates the structural integrity of trabecular bone and the efficiency of bone remodeling, serving as a key marker of osteogenic activity. In our study, the Piezo1-treated group showed a significant increase in BMD and Tb.Th at both 6 and 8 weeks, suggesting that Piezo1 effectively promotes trabecular mineralization and structural maturation. This enhancement is likely associated with Piezo1-mediated mechano-transduction, which stimulates the osteogenic differentiation of BM-MSCs and promotes bone matrix deposition. Specifically, the activation of Piezo1 upregulates the expression of osteogenesis-related factors such as Runx2, COL-1, and OCN, thereby accelerating new bone formation and mineralization, and improving both the density and structural quality of bone tissue.

In terms of biochemical indicators, we assessed the serum levels of ALP and TGF-β1 in the rats. ALP is an important marker of bone formation, while TGF-β1 plays an essential role in the bone healing process. We observed that the levels of ALP and TGF-β1 in the Piezo1 group were significantly higher than those in the fracture group at weeks 6 and 8, indicating that Piezo1 accelerates bone

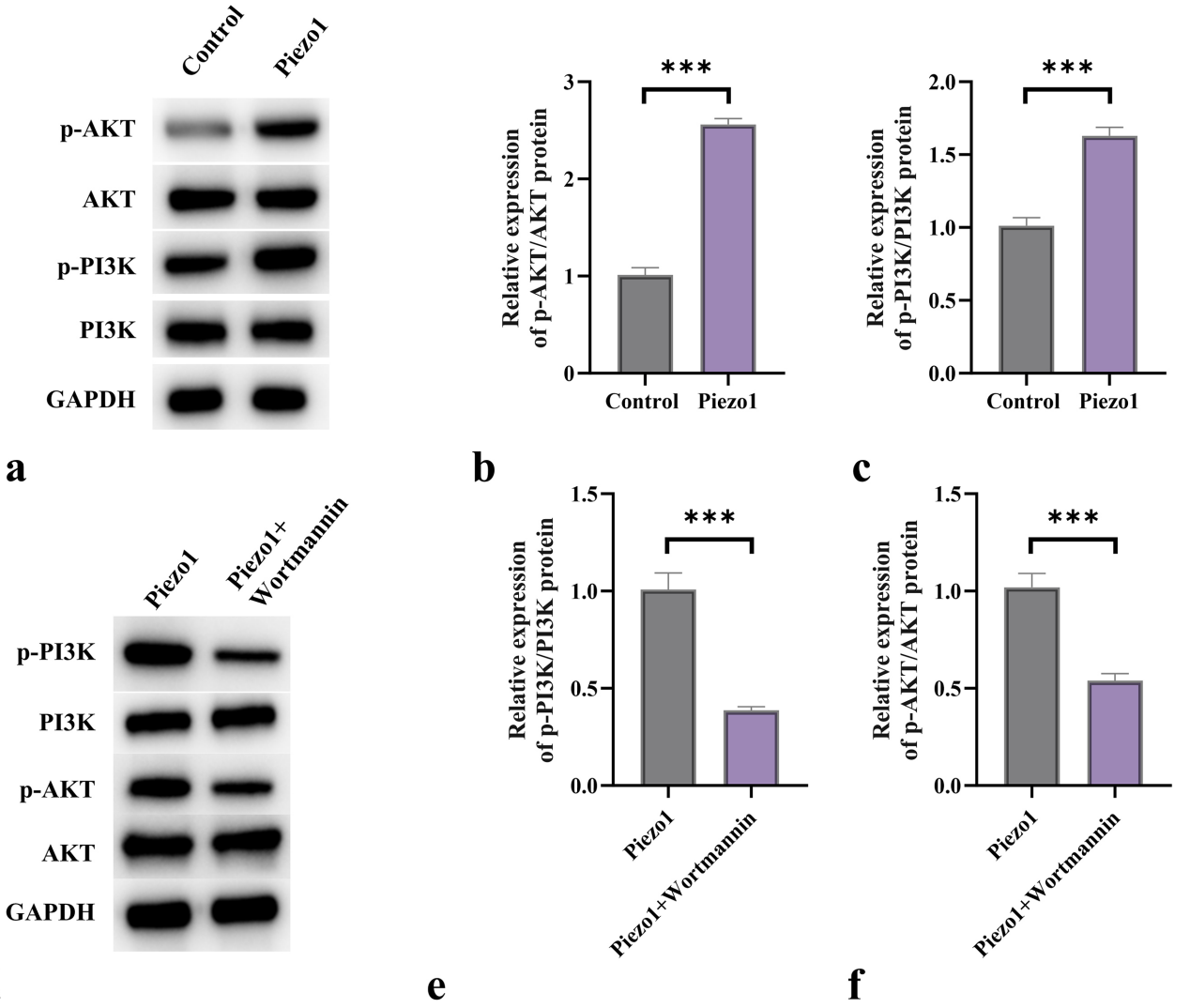

Fig. 5. Piezo1 activates the Phosphoinositide 3-kinase/Protein kinase B (PI3K/AKT) signaling pathway in BM-MSCs. (a–c) Protein expression levels of p-AKT, AKT, p-PI3K, and PI3K in BM-MSCs treated with Piezo1. (d–f) Protein expression levels of p-AKT, AKT, p-PI3K, and PI3K in BM-MSCs after treatment with Piezo1 and Wortmannin. n = 3. ***$p < 0.001$.

healing by promoting the expression of osteogenic factors. Consistent with our findings, Li *et al.* [22] investigated the significance of TGF-β1 in the proliferation and differentiation of osteoblasts, underscoring its role in bone healing. Hence, Piezo1 may accelerate bone healing by enhancing osteoblast activity and promoting the expression of bone-related factors.

The histological assessment demonstrated that the fracture group primarily showed fibrous and cartilaginous tissues at week 6, whereas the Piezo1 group exhibited mature bone tissue at an earlier stage. This finding is coherent with the literature describing the stages of bone fracture healing, indicating that Piezo1 not only accelerates bone healing but also improves the quality of bone tissue. Studies have demonstrated that changes in tissue types during the bone healing process significantly influence the overall quality of healing [23,24]. The application of Piezo1 may enhance the final healing outcome by promoting the formation of early bone tissue.

BMP-2 plays a crucial role in osteogenic differentiation, and our immunohistochemical analysis revealed that the expression level of BMP-2 in the Piezo1 group was notably higher than in the fracture group. This result aligns with previous studies emphasizing the essential role of BMP-2 in bone healing [25,26]. BMP-2 directly influences the efficiency of bone healing by stimulating the differentiation and mineralization of osteoblasts. Our findings suggest that Piezo1 may enhance the osteogenic capability of BM-MSCs by regulating BMP-2 expression.

We further explored the impact of Piezo1 on the PI3K/AKT signaling pathway in BM-MSCs. The results revealed that Piezo1 significantly elevated the phosphorylation levels of PI3K and AKT in BM-MSCs in contrast to the control group. This finding aligns with Zhan *et al.* [27] and

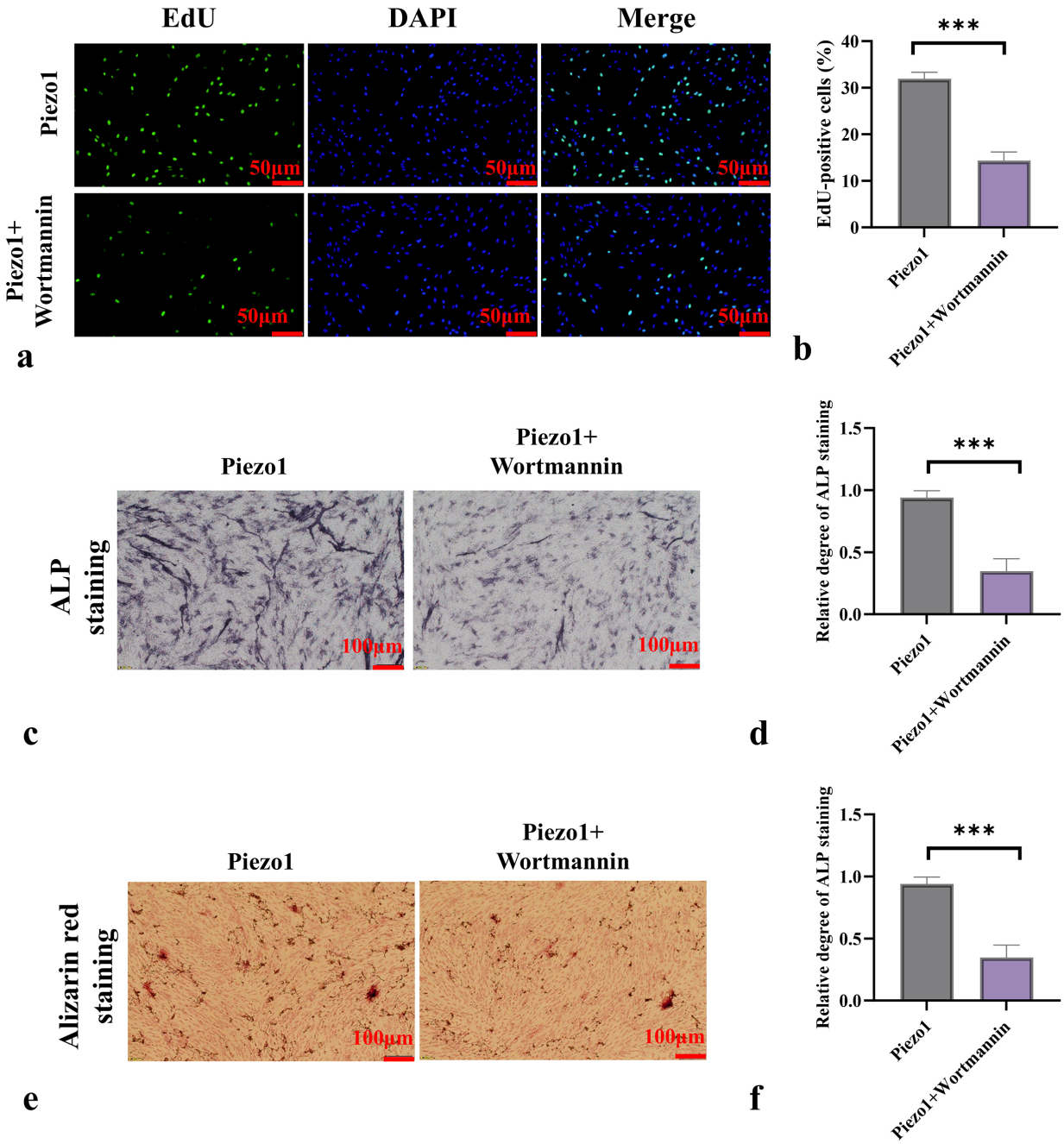

Fig. 6. Piezo1 promotes the proliferation and osteogenic differentiation of BM-MSCs by activating the PI3K/AKT signaling pathway. (a,b) Levels of 5-Ethynyl-2′-deoxyuridine (EdU)-positive cells in BM-MSCs after treatment with Piezo1 and Wortmannin. (c,d) ALP staining results of BM-MSCs after treatment with Piezo1 and Wortmannin. (e,f) Alizarin Red staining results of BM-MSCs after treatment with Piezo1 and Wortmannin. n = 3. ***$p < 0.001$.

Chen *et al.* [28], which reported the role of the PI3K/AKT pathway in promoting osteoblast function. Our observations suggest that Piezo1 may enhance osteoblast functionality by activating this signaling pathway. The PI3K/AKT pathway not only promotes osteogenic differentiation but also inhibits cell apoptosis, thereby providing a favorable microenvironment for bone healing.

In the high-concentration (10 μm) Piezo1-treated group, BM-MSCs exhibited significant cytotoxicity. This finding suggested that the therapeutic window for Piezo1 must be carefully determined to ensure its bone healing-promoting effects are not compromised by cytotoxicity. Future studies should emphasize identifying the optimal dosage of Piezo1 and investigating its mechanisms of action on osteoblasts to reduce potential cytotoxic effects.

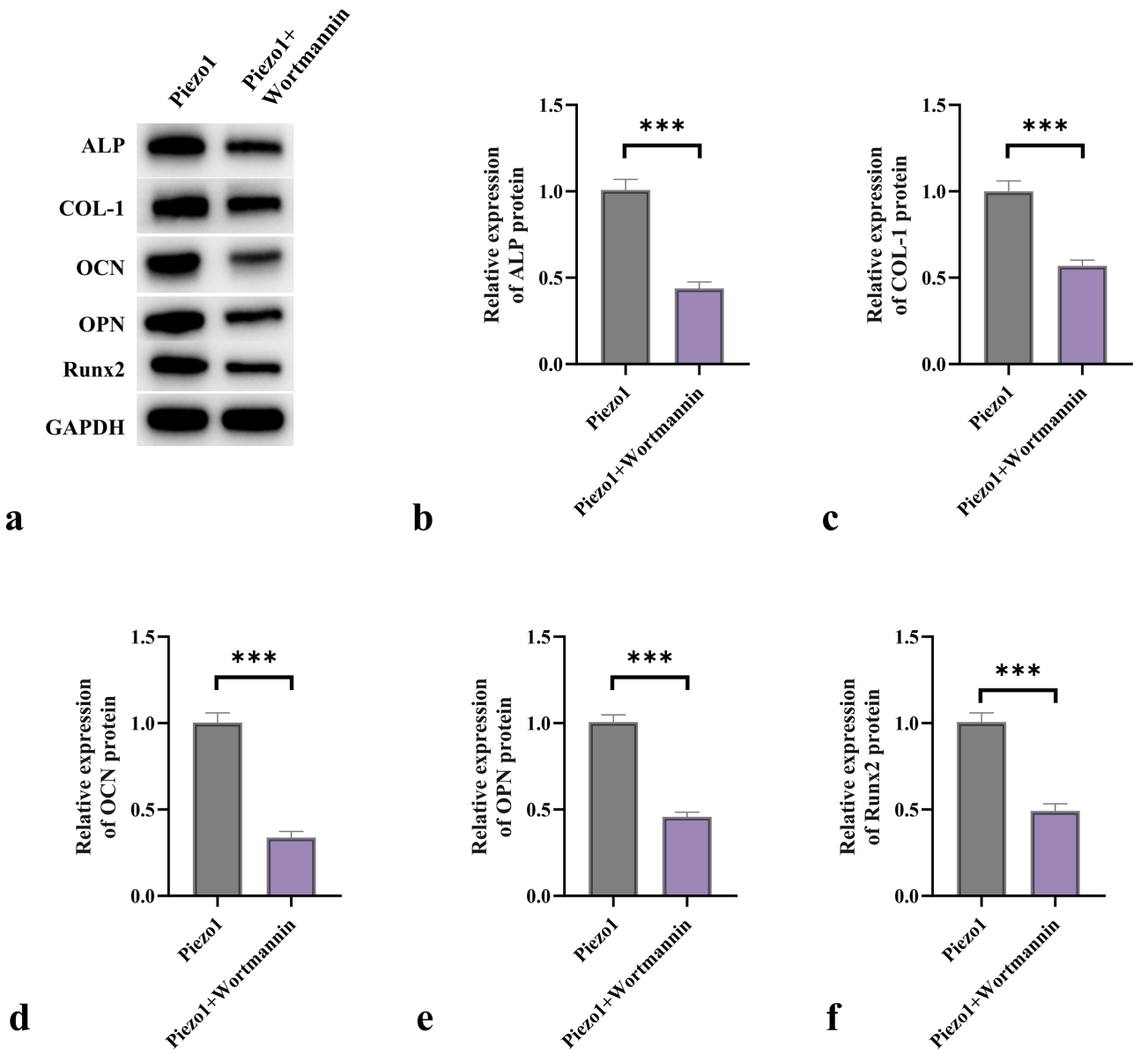

Fig. 7. Piezo1 enhances the expression of osteogenic genes in BM-MSCs through activation of the PI3K/AKT signaling pathway. (a–f) Protein expression levels of ALP, COL-1, OCN, OPN, and Runx2 in BM-MSCs after treatment with Piezo1 and Wortmannin. n = 3. ***$p < 0.001$.

In summary, the results of our study align well with existing literature, underscoring the multiple mechanisms by which Piezo1 promotes fracture healing. Piezo1 not only accelerates bone healing by promoting the proliferation and differentiation of osteoblasts but may also improve the quality of bone repair by regulating the expression of essential biomarkers. These findings provide a solid theoretical basis for Piezo1 as a potential bone healing promoter, warranting further validation in preclinical and clinical studies.

Despite several valuable findings, we acknowledge some limitations in our study. First, although the involvement of the PI3K/AKT signaling pathway in Piezo1-mediated osteogenic differentiation was demonstrated *in vitro* using Wortmannin, *in vivo* experiments with pathway inhibitors were not performed, limiting a deeper understanding of Piezo1's molecular mechanisms under physiological conditions. Second, a Wortmannin-only group was not included to evaluate its independent effects on BM-MSC proliferation and differentiation. While its inhibitory role has been reported in previous studies, the specific effects of this in our study remain unclear. Additionally, this study focused solely on the PI3K/AKT pathway and did not investigate other potential signaling pathways associated with Piezo1, such as Mitogen-Activated Protein Kinase (MAPK) or Wnt pathways. The *in vitro* assessments of osteogenic differentiation were conducted over a rela-

tively short duration, and long-term studies are needed to confirm functional bone formation. Finally, using a rat fracture model and mouse recombinant proteins may introduce species differences that could affect the translational significance of these findings to human bone biology.

This study demonstrates that Piezo1 promotes osteogenic differentiation of bone marrow-derived mesenchymal stem cells by activating the PI3K/AKT pathway, indicating its potential to enhance bone healing. Clinically, Piezo1 holds promise for accelerating fracture repair and bone regeneration. In addition to demonstrating the osteogenic effects of Piezo1 recombinant protein, this study provides preliminary insight into its potential for clinical translation. The selected dose of 100 mg/kg was determined based on prior dose–response screening, which identified it as the most effective concentration for enhancing bone regeneration without observable systemic toxicity in rats. However, we acknowledge that this study did not include comprehensive toxicological assessments—such as histological evaluation of major organs or measurement of systemic inflammatory markers—which represent a limitation to be addressed in future research. To mitigate the risks associated with systemic administration and improve therapeutic precision, future studies should explore localized delivery systems. These may include injectable hydrogels, biodegradable scaffolds, or slow-release microsphere formulations, which enable sustained, site-specific release of Piezo1 protein at the fracture site. Such delivery strategies could reduce off-target effects and systemic exposure, thereby enhancing the safety and feasibility of Piezo1-based therapies in clinical applications.

In our *in vitro* experiments, while Piezo1 promoted BM-MSC viability and osteogenic differentiation in a dose-dependent manner within a certain range, we observed a plateau or slight decline in cell activity at the highest concentration, which may indicate potential cytotoxic effects or cellular adaptation. However, several challenges remain for clinical translation. Optimization of dose and treatment duration is needed to ensure both safety and efficacy. Additionally, efficient, targeted, and sustained delivery systems—such as scaffolds or nanoparticle carriers—must be developed. Moreover, a systematic evaluation of Piezo1's immunogenicity and potential side effects is essential to guarantee its safety. Future research should focus on addressing these challenges to advance the clinical application of Piezo1 in bone repair. Research could also explore the efficacy of Piezo1 in different types of fractures and stages of healing, as well as its combined effects with other bone-healing promoters. Given the widespread availability of Piezo1, its accessibility and safety in clinical applications must be considered. These efforts will help establish clinical strategies for Piezo1 in bone healing treatments, providing effective solutions for fracture patients.

Conclusions

This study underscores the role of Piezo1 in promoting fracture healing by enhancing osteoblast growth and differentiation, as well as improving bone repair quality through key biomarkers, including ALP, TGF-β1, and BMP-2. Additionally, Piezo1 activates the PI3K/AKT signaling pathway, thereby boosting the osteogenic potential of BM-MSCs.

Availability of Data and Materials

The data that support the findings of this study are available from the corresponding author upon reasonable request.

Author Contributions

SKM and HLT designed the research study. SKM, XLQ, HXH and HLT performed the research. SKM and HLT collected and analyzed the data. SKM, XLQ, HXH and HLT have been involved in drafting the manuscript and all authors have been involved in revising it critically for important intellectual content. All authors give final approval of the version to be published. All authors have participated sufficiently in the work to take public responsibility for appropriate portions of the content and agreed to be accountable for all aspects of the work in ensuring that questions related to its accuracy or integrity.

Ethics Approval and Consent to Participate

Protocol was approved by the Institutional Animal Care and Use Committee of Shandong Academy of Pharmaceutical Sciences (IACUC-care-2024024) in accordance with Guide for the Care and Use of Laboratory Animals, 8th edition (National Research Council (NRC), 2010).

Acknowledgment

Not applicable.

Funding

This research received no external funding.

Conflict of Interest

The authors declare no conflict of interest.

References

[1] Wildemann B, Ignatius A, Leung F, Taitsman LA, Smith RM, Pesántez R, *et al*. Non-union bone fractures. Nature Reviews. Disease Primers. 2021; 7: 57. https://doi.org/10.1038/s41572-021-00289-8.

[2] Molitoris KH, Huang M, Baht GS. Osteoimmunology of Frac-

ture Healing. Current Osteoporosis Reports. 2024; 22: 330–339. https://doi.org/10.1007/s11914-024-00869-z.

[3] Chun YS, Lee DH, Won TG, Kim Y, Shetty AA, Kim SJ. Current Modalities for Fracture Healing Enhancement. Tissue Engineering and Regenerative Medicine. 2022; 19: 11–17. https://doi.org/10.1007/s13770-021-00399-0.

[4] Zhang H, Wang R, Wang G, Zhang B, Wang C, Li D, *et al*. Single-Cell RNA Sequencing Reveals B Cells Are Important Regulators in Fracture Healing. Frontiers in Endocrinology. 2021; 12: 666140. https://doi.org/10.3389/fendo.2021.666140.

[5] Gürbüz K, Yerer MB, Gürbüz P, Halıcı M. Icariin promotes early and late stages of fracture healing in rats. Eklem Hastaliklari Ve Cerrahisi = Joint Diseases & Related Surgery. 2019; 30: 282–288. https://doi.org/10.5606/ehc.2019.66796.

[6] Maruyama M, Rhee C, Utsunomiya T, Zhang N, Ueno M, Yao Z, *et al*. Modulation of the Inflammatory Response and Bone Healing. Frontiers in Endocrinology. 2020; 11: 386. https://doi.org/10.3389/fendo.2020.00386.

[7] Lai A, Cox CD, Chandra Sekar N, Thurgood P, Jaworowski A, Peter K, *et al*. Mechanosensing by Piezo1 and its implications for physiology and various pathologies. Biological Reviews of the Cambridge Philosophical Society. 2022; 97: 604–614. https://doi.org/10.1111/brv.12814.

[8] Zhou T, Gao B, Fan Y, Liu Y, Feng S, Cong Q, *et al*. Piezo1/2 mediate mechanotransduction essential for bone formation through concerted activation of NFAT-YAP1-ß-catenin. eLife. 2020; 9: e52779. https://doi.org/10.7554/eLife.52779.

[9] Mukhopadhyay A, Tsukasaki Y, Chan WC, Le JP, Kwok ML, Zhou J, *et al*. trans-Endothelial neutrophil migration activates bactericidal function via Piezo1 mechanosensing. Immunity. 2024; 57: 52–67.e10. https://doi.org/10.1016/j.immuni.2023.11.007.

[10] Wang J, Sun YX, Li J. The role of mechanosensor Piezo1 in bone homeostasis and mechanobiology. Developmental Biology. 2023; 493: 80–88. https://doi.org/10.1016/j.ydbio.2022.11.002.

[11] Guan H, Wang W, Jiang Z, Zhang B, Ye Z, Zheng J, *et al*. Magnetic Aggregation-Induced Bone-Targeting Nanocarrier with Effects of Piezo1 Activation and Osteogenic-Angiogenic Coupling for Osteoporotic Bone Repair. Advanced Materials (Deerfield Beach, Fla.). 2024; 36: e2312081. https://doi.org/10.1002/adma.202312081.

[12] Liu Y, Tian H, Hu Y, Cao Y, Song H, Lan S, *et al*. Mechanosensitive Piezo1 is crucial for periosteal stem cell-mediated fracture healing. International Journal of Biological Sciences. 2022; 18: 3961–3980. https://doi.org/10.7150/ijbs.71390.

[13] Qin L, He T, Chen S, Yang D, Yi W, Cao H, *et al*. Roles of mechanosensitive channel Piezo1/2 proteins in skeleton and other tissues. Bone Research. 2021; 9: 44. https://doi.org/10.1038/s41413-021-00168-8.

[14] Tan J, Li J, Cao B, Wu J, Luo D, Ran Z, *et al*. Niobium promotes fracture healing in rats by regulating the PI3K-Akt signalling pathway: An *in vivo* and *in vitro* study. Journal of Orthopaedic Translation. 2022; 37: 113–125. https://doi.org/10.1016/j.jot.2022.08.007.

[15] Wang C, Wang X, Cheng H, Fang J. MiR-22-3p facilitates bone marrow mesenchymal stem cell osteogenesis and fracture healing through the SOSTDC1-PI3K/AKT pathway. International Journal of Experimental Pathology. 2024; 105: 52–63. https://doi.org/10.1111/iep.12500.

[16] Liu Z, Li Y, Yang J, Huang J, Luo C, Zhang J, *et al*. Bone morphogenetic protein 9 enhances osteogenic and angiogenic responses of human amniotic mesenchymal stem cells cocultured with umbilical vein endothelial cells through the PI3K/AKT/mTOR signaling pathway. Aging. 2021; 13: 24829–24849. https://doi.org/10.18632/aging.203718.

[17] Wen C, Wang XJ, Han JC, Wang HW. Comparative study of the effects of intramedullary nail fixation and minimally invasive percutaneous plate internal fixation technique on platelet activation and serum transforming growth factor-β1(TGF-β) 1 and bone morphogenetic protein-2 (BMP-2) in patients with tibial and fibular fracture. Zhongguo Gu Shang = China Journal of Orthopaedics and Traumatology. 2023; 36: 1100–1106. https://doi.org/10.12200/j.issn.1003-0034.2023.11.018. (In Chinese)

[18] Jann J, Gascon S, Roux S, Faucheux N. Influence of the TGF-β Superfamily on Osteoclasts/Osteoblasts Balance in Physiological and Pathological Bone Conditions. International Journal of Molecular Sciences. 2020; 21: 7597. https://doi.org/10.3390/ijms21207597.

[19] Purbantoro SD, Osathanon T, Nantavisai S, Sawangmake C. Osteogenic growth peptide enhances osteogenic differentiation of human periodontal ligament stem cells. Heliyon. 2022; 8: e09936. https://doi.org/10.1016/j.heliyon.2022.e09936.

[20] Li Y, Fu G, Gong Y, Li B, Li W, Liu D, *et al*. BMP-2 promotes osteogenic differentiation of mesenchymal stem cells by enhancing mitochondrial activity. Journal of Musculoskeletal & Neuronal Interactions. 2022; 22: 123–131.

[21] Kang T, Yang Z, Zhou M, Lan Y, Hong Y, Gong X, *et al*. The role of the Piezo1 channel in osteoblasts under cyclic stretching: A study on osteogenic and osteoclast factors. Archives of Oral Biology. 2024; 163: 105963. https://doi.org/10.1016/j.archoralbio.2024.105963.

[22] Li J, Ge L, Zhao Y, Zhai Y, Rao N, Yuan X, *et al*. TGF-β2 and TGF-β1 differentially regulate the odontogenic and osteogenic differentiation of mesenchymal stem cells. Archives of Oral Biology. 2022; 135: 105357. https://doi.org/10.1016/j.archoralbio.2022.105357.

[23] Palanisamy P, Alam M, Li S, Chow SKH, Zheng YP. Low-Intensity Pulsed Ultrasound Stimulation for Bone Fractures Healing: A Review. Journal of Ultrasound in Medicine: Official Journal of the American Institute of Ultrasound in Medicine. 2022; 41: 547–563. https://doi.org/10.1002/jum.15738.

[24] Zhang L, Jiao G, Ren S, Zhang X, Li C, Wu W, *et al*. Exosomes from bone marrow mesenchymal stem cells enhance fracture healing through the promotion of osteogenesis and angiogenesis in a rat model of nonunion. Stem Cell Research & Therapy. 2020; 11: 38. https://doi.org/10.1186/s13287-020-1562-9.

[25] Zhou L, Wang J, Mu W. BMP-2 promotes fracture healing by facilitating osteoblast differentiation and bone defect osteogenesis. American Journal of Translational Research. 2023; 15: 6751–6759.

[26] Wei Q, Holle A, Li J, Posa F, Biagioni F, Croci O, *et al*. BMP-2 Signaling and Mechanotransduction Synergize to Drive Osteogenic Differentiation via YAP/TAZ. Advanced Science (Weinheim, Baden-Wurttemberg, Germany). 2020; 7: 1902931. https://doi.org/10.1002/advs.201902931.

[27] Zhan H, Xie D, Yan Z, Yi Z, Xiang D, Niu Y, *et al*. Fluid shear stress-mediated Piezo1 alleviates osteocyte apoptosis by activating the PI3K/Akt pathway. Biochemical and Biophysical Research Communications. 2024; 730: 150391. https://doi.org/10.1016/j.bbrc.2024.150391.

[28] Chen P, Zhang G, Jiang S, Ning Y, Deng B, Pan X, *et al*. Mechanosensitive Piezo1 in endothelial cells promotes angiogenesis to support bone fracture repair. Cell Calcium. 2021; 97: 102431. https://doi.org/10.1016/j.ceca.2021.102431.